Molecules and Cells

Retinoid Metabolism in the Degeneration of Pten-Deficient Mouse Retinal Pigment Epithelium

You-Joung Kim[1], Sooyeon Park[1], Taejeong Ha[1], Seungbeom Kim[1], Soyeon Lim[1], Han You[2], and Jin Woo Kim[1,*]

[1]Department of Biological Sciences, Korea Advanced Institute of Science and Technology (KAIST), Daejeon 34141, Korea, [2]School of Life Sciences, Xiamen University, Xiamen 361005, China
*Correspondence: jinwookim@kaist.ac.kr
https://doi.org/10.14348/molcells.2021.0138
www.molcells.org

In vertebrate eyes, the retinal pigment epithelium (RPE) provides structural and functional homeostasis to the retina. The RPE takes up retinol (ROL) to be dehydrogenated and isomerized to 11-*cis*-retinaldehyde (11-*cis*-RAL), which is a functional photopigment in mammalian photoreceptors. As excessive ROL is toxic, the RPE must also establish mechanisms to protect against ROL toxicity. Here, we found that the levels of retinol dehydrogenases (RDHs) are commonly decreased in *phosphatase tensin homolog* (*Pten*)-deficient mouse RPE, which degenerates due to elevated ROL and that can be rescued by feeding a ROL-free diet. We also identified that *RDH* gene expression is regulated by forkhead box O (FOXO) transcription factors, which are inactivated by hyperactive Akt in the *Pten*-deficient mouse RPE. Together, our findings suggest that a homeostatic pathway comprising PTEN, FOXO, and RDH can protect the RPE from ROL toxicity.

Keywords: forkhead box O, phosphatase tensin homolog, phosphoinositide 3-kinase-Akt pathway, retinal pigment epithelium, retinoids

INTRODUCTION

Light, which carries high energy, is an essential component for living organisms. However, it also generates various reactive oxidative materials that can damage cellular macromolecules, such as nucleic acids, proteins, and lipids (Putting et al., 1992). Light-induced damage is a particularly serious threat for vertebrate photoreceptors, which absorb light photons using the photopigments in their outer segments (OS) and transduce electrochemical signals to inner retinal neurons. A photo-damaged, non-functional photoreceptor OS is quickly eliminated by the retinal pigment epithelium (RPE) through phagocytic ingestion and replaced with a new OS to ensure the proper visual functions of photoreceptors (Garita-Hernandez et al., 2019). However, whereas OS undergo daily renewal, the RPE undergoes relatively minimal regeneration in mammals; over time, the accumulation of damaged photoreceptor components will, therefore, cause the RPE to degenerate. This can lead to retinal degenerative diseases, such as age-related macular degeneration (AMD), which is a leading cause of blindness in aged populations (Kang et al., 2009).

In degenerating RPE, many oxidative materials are accumulated. Lipofuscins, which are yellow-brown pigment granules composed of oxidized lipids, are frequently detectable in the aged RPE (Parish et al., 1998). Similar observations can be made in patients with Stargardt disease, who accumulate *bis*-retinoid A2E in their photoreceptors and lipofuscins in RPE cells that have phagocytized A2E-containing photoreceptor OS (Radu et al., 2004). Defective retinoid metabolism has also been reported in other retinal degenerative diseases. For example, Leber congenital amaurosis (LCA) is a retinal degenerative disease caused by mutations in lecithin-retinol ac-

Received 31 May, 2021; revised 4 June, 2021; accepted 7 June, 2021; published online 11 August, 2021

eISSN: 0219-1032

yltransferase (LRAT), which converts *all-trans*-retinol (*at*-ROL) received from the photoreceptors to *all-trans*-retinyl ester (*at*-RE) in the RPE (Saari et al., 1993) (Fig. 1A). The *at*-RE is then converted to 11-*cis*-ROL by RPE-specific 65-kDa protein (RPE65) for subsequent oxidation to 11-*cis*-retinaldehyde (11-*cis*-RAL), which is the functional photopigment used in human photoreceptors (Jin et al., 2005; Redmond et al., 1998). Mutations of *RPE65* have been identified in some patients with LCA and retinitis pigmentosa (RP) (Bainbridge et al., 2008; Morimura et al., 1998). Therefore, *at*-ROL, which is the substrate of LRAT, and *at*-RE, which is the substrate of RPE65, accumulate in the RPE of patients carrying mutations in the *LRAT* and *RPE65* genes, respectively, and could cause RPE degeneration (Imanishi et al., 2004; Sahu and Maeda, 2016).

Retinoids also contribute to many developmental and homeostatic events; for this purpose, they are converted to retinoic acid (RA), which binds its receptor to induce the expression of many important regulatory genes directly (Leid et al., 1992; Niederreither and Dolle, 2008). Thus, insufficient production of RA results in many health problems, including malformation of organs, growth of neoplastic tissue, and disturbance of the immune system (Cunningham and Duester, 2015).

Animals should take up ROL in their diet as vitamin A (VitA) or carotenoids like β-carotene, which can be broken into two RAL molecules for subsequent conversion to ROL by β-carotene dioxygenase 1 (BCO1) (Ferreira et al., 2020; von Lintig and Vogt, 2000). Insufficient intake of VitA and/or carotenoids therefore causes various health problems, including night blindness, xerophthalmia, hyperkeratosis, increased susceptibility to severe infection, and so on (Maden, 2002; Sommer, 2008). However, excessive ROL is also harmful to cells (DiPalma and Ritchie, 1977); thus, an optimal intake is needed.

In healthy cells, enzymes that convert ROL to RAL and then to RA are expressed to avoid of overaccumulation of ROL and RAL derivatives. The conversion of RAL to RA is carried out by retinaldehyde dehydrogenases (RALDHs), while the conversion of ROL to RAL is mediated by retinol dehydrogenases (RDHs) (Ferreira et al., 2020; Liden and Eriksson, 2006). These enzymes are especially high in hepatocytes and cells of the RPE, which actively metabolize ROL and RAL. Retinoid metabolism in the latter cell type plays a unique role in the visual system, whereas that in the former cell type plays a more general role in detoxification (Pares et al., 2008).

MATERIALS AND METHODS

Mice

Pten-flox mice, in which two *loxP* sequences are inserted into the intron 3 and 5 of *Pten* gene, were bred with *TRP1-Cre* mice, which express Cre recombinase under the promoter sequences of *human tyrosinase related protein 1* (*TRP1*), to generate $Pten^{flox/flox}$;*TRP1-Cre* (*Pten-cko*) mice as it was described previously (Kim et al., 2008). Mice were fed with the VitA-enriched (ROL(+)) chow (ENVIGO, 2018S), the VitA-deficient (ROL(–)) chow (ENVIGO, TD.86143), or the VitA-deficient;β-carotene (100 mg/kg) chow after weaning at post-natal day 21 (P21). To supply RA, the mice were injected *at*-RA (Sigma, USA), which was dissolved in DMSO and mixed in corn oil (20 mg *at*-RA/kg body weight), once in every other day beginning at P21 and continuing for 1 month. All experiments using the mice were carried out according to the guidance of Institutional Animal Care and Use Committee (IACUC) of Korea Advanced Institute of Science and Technology (KAIST) (No. KA2011-37). All mice used in this study were maintained in a specific pathogen-free facility of KAIST Laboratory Animal Resource Center.

Western blot (WB) analysis

Mouse RPE and retina were isolated from the mice as it was described previously (Kim et al., 2008). The cell lysates (70 μg proteins) were analyzed by SDS-PAGE prior to the transfer onto polyvinylidene difluoride (PVDF) membrane for subsequent WB. Corresponding proteins on the PVDF membranes were detected by anti-ADH1 (1:500; Abcam, UK), anti-ADH7 (1:500; Abcam), anti-RDH5 (1:500; Abcam), anti-RDH10 (1:500; MyBioSource, USA), anti-PTEN (1:500; Cell Signaling Technology, USA), anti-RPE65 (1:500; Abcam), anti-FOXO1 (1:500; Cell Signaling Technology), anti-FOXO3a (1:500; Cell Signaling Technology), anti-FOXO4 (1:500; Cell Signaling Technology), anti-pFOXO1(Thr24)/pFOXO3a(Thr32) (1:500; Cell Signaling Technology), anti-pAKT(T308) (1:500; Cell Signaling Technology), and anti-β-actin (1:2,000; Santa Cruz Biotechnology, USA). The antibodies bound to the proteins on the blots were visualized by the incubation in SuperSignal™ West Pico Chemiluminescent Substrate or SuperSignal™ West Femto Maximum Sensitivity Substrate (Thermo Fisher Scientific, USA) after incubating with secondary antibodies, which were conjugated with horseradish peroxidase (HRP) and recognize the primary antibodies listed above.

Measurement of ROL and RA concentration

Mouse RPE and retina were collected from 20 mouse eyes and were immediately placed in brown tubes and immersed in liquid nitrogen to minimize the degeneration and modification of ROL and RA. After homogenization in ice-cold phosphate-buffered saline (PBS; pH 7.2) using Dounce homogenizer, the cell suspension was subjected to sonication prior to the centrifugation at 1,500*g* for 15 min. Concentrations of ROL and RA were measured by the Mouse Vitamin A ELISA Kit (MBS722364 [MyBioSource, USA]; mainly detect ROL) and Mouse Retinoic Acid ELISA Kit (MBS706971; MyBioSource) following the manufacturer's instruction.

Cell culture and luciferase assay

Human embryonic kidney 293T were cultured in Dulbecco's modified Eagle's medium (DMEM) supplemented with 10% fetal bovine serum (FBS; Gibco, USA) and were transfected with pGL3 luciferase reporter plasmids by polyethylenimine transfection method. The cells were also co-transfected with pSV-β-galactosidase plasmid in the same amount of pGL3 reporter plasmids. The cell extracts were prepared after 24 h and assessed for luciferase activity followed by the normalization with β-galactosidase activity values.

Eye section and immunohistochemistry

After anaesthetizing by intraperitoneal injection of tribromoethanol (Avertin; Sigma), the mice were perfused with PBS (pH 7.5) containing 0.1% heparin (Millipore, USA) and then with 4% paraformaldehyde (PFA; Sigma) in PBS. The eyes were isolated from the mice and fixed further in 4% PFA/PBS solution at 4°C for 2 h. The samples were moved into 20% sucrose/PBS solution overnight at 4°C prior to embedding in the TissueTek OCT compound (Sakura Finetek, USA). The frozen eyes were then cryosectioned on the Superfrost glass slides (14 μm thickness) using Leica cryostat (CM1860; Leica, Germany).

For immunohistochemistry, the sections were blocked with 5% normal donkey serum and 5% normal goat serum in PBS containing 0.2% Triton X-100 before incubating with primary antibodies at room temperature for 2 h. Mouse monoclonal antibodies against Ezrin (1:200; Invitrogen, USA) and Rhodopsin (1:200; Millipore); rabbit polyclonal antibodies against FOXO3a (1:200; Cell Signaling Technology), GFAP (1:200; Abcam), Otx2 (1:200; Abcam), GS (1:200; Sigma), and β-catenin (1:200; Cell Signaling Technology); goat polyclonal antibodies against Sox2 (1:200; Santa Cruz Biotechnology) were incubated at 4°C for overnight. Fluorescent images were obtained with a confocal microscope (Fluoview FV1000 and FV3000; Olympus, Japan) after staining the sections with Cy3 and Alexa488-conjugated secondary antibodies at room temperature for 1 h.

Chromatin immunoprecipitation (ChIP)

Mouse RPE and retina were isolated from P60 mice and protein-DNA complexes were immunoprecipitated with rabbit preimmune IgG or rabbit anti-FOXO3a IgG in the procedures reported previously (Moon et al., 2018). Quantitative polymerase chain reaction (qPCR) was performed with the immunoprecipitated DNA using SYBR Green (Applied Biosystems, USA) with designed primers to upstream region containing FOXO binding sequences of *Adh1* (forward 5'-CCCAACAGCACTCGTCCA-3', reverse 5'-CTTCCCTCCTCTAGTGAACCG-3'), *Adh7* (forward 5'-CCCATCTCCATCGCCATTACT-3', reverse 5'-ATCCGGTCTCCGTTCTTAGC-3'), and *Rdh10* (forward 5'-CTAACTCGCGGCTGTCACC-3', reverse 5'-CGATCCGGACGCGAAGG-3').

Identification of evolutionary conserved regions (ECRs)

The analysis of ECRs in genomes of various species was performed in the ECR browser website (https://ecrbrowser.dcode.org/ecrInstructions/ecrInstructions.html). A base genome was mouse and parameter set in default value (minimum length of ECRs, 100 bp; identity of ECRs, 70%). Possible consensus sequences site recognized by FOXO were marked with yellow stars: 5′-GTAAA(T/C)AA-3′, known as the Daf-16 family member-binding element (DBE) and 5′-(C/A)(A/C)AAA(C/T)AA-3′, known as the insulin-responsive sequence (IRE). All FOXO-family members recognize the core sequence 5'-(A/C)AA(C/T)A-3' (Obsil and Obsilova, 2011).

Statistical analysis

Statistical analysis was performed by Prism 9 software (GraphPad, USA). Data from statistical analysis are presented as the mean ± SD. Student's *t*-test was used to determine the significant difference between two groups. *P* values were calculated using a two-tailed unpaired *t*-test. *P* value < 0.05 was considered statistically significant.

RESULTS

Retinoid metabolism enzyme expression is reduced in Pten-deficient mouse RPE

We previously reported that the mouse RPE is degenerated upon genetic and physiological inactivation of *Pten* (Kim et al., 2008; Lee et al., 2011), which is a negative regulator of the phosphoinositide 3-kinase (PI3K) and Akt pathway (Stambolic et al., 1998). The genes whose mRNA levels exhibited significant decreases in *Pten*-deficient mouse RPE included those encoding both classical retinol dehydrogenases (*Rdh5* and *Rdh10*) and non-classical retinol dehydrogenases (short chain alcohol dehydrogenases, *Adh1* and *Adh7*) (Kim et al., 2008). Here, to experimentally validate these changes, we compared the mRNA and protein levels of these enzymes in P21 *TRP1-Cre* and *Pten-cko* littermate mouse RPE by real-time PCR (RT-PCR) and WB, respectively (see the information of the mice in Materials and Methods section). We found that the mRNA and protein levels of Adh and Rdh in *Pten-cko* mouse RPE were significantly lower than those in *TRP1-Cre* littermate mouse RPE (Figs. 1A-1C). We also found that the level of Lrat, which converts *at*-ROL obtained from the photoreceptor OS to *at*-RE in the RPE (Saari and Bredberg, 1989), was also decreased in the *Pten-cko* mouse RPE, whereas the expression of Rpe65, which is responsible for converting *at*-RE to 11-*cis*-ROL in the RPE (Jin et al., 2005), was not changed significantly (Figs. 1A-1C). The results suggest that the expression of those retinoid metabolism-related enzymes in mouse RPE is regulated by a mechanism that is sensitive to Pten.

As we hypothesized that the altered expression levels of those *Rdh* genes would change the contents of retinoids in the RPE, we examined the levels of ROL and RA in the mouse RPE. Consistent with the decreased expression of *Rdh* and *Lrat*, the level of ROL, a precursor of RAL and RE, was significantly increased in P21 *Pten*-deficient RPE compared to *TRP1-Cre* littermate mouse RPE (Fig. 1D). On the contrary, the level of RA, a metabolic product of RAL, was decreased in the *Pten*-deficient mouse RPE (Fig. 1E). These results suggest that the metabolic flow of ROL-RAL-RA is ineffective in the *Pten*-deficient mouse RPE due to the reduced *Rdh* expression.

Degeneration of Pten-deficient mouse RPE does not arise from a decrease of RA

Given the importance of RA-dependent gene expression for cell survival (Michalik and Wahli, 2007), we speculated that a decrease of RA could be correlated with the degeneration of the *Pten*-deficient RPE. We, thus, tested this by increasing RA in the mouse RPE. In practical, we supplemented *TRP1-Cre* and *Pten-cko* littermate mice with *at*-RA via intraperitoneal injection once in every other day beginning at P21 and continuing for 1 month, and investigated whether this protected the RPE from degeneration in *Pten-cko* mouse eyes.

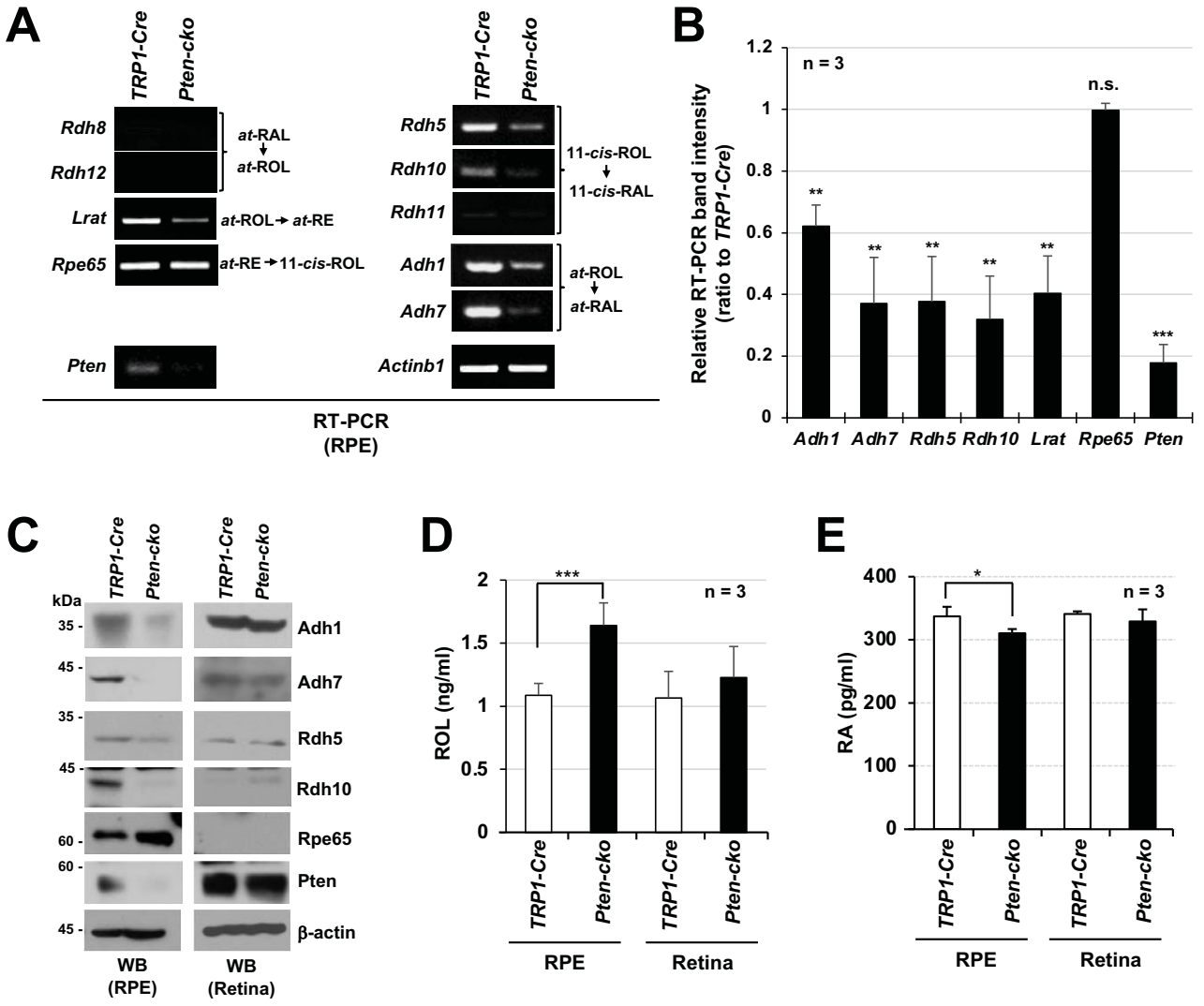

Fig. 1. Decrease of retinoid metabolism enzymes in *Pten-cko* mouse RPE. (A) Relative levels of mRNA of retinoid metabolism enzymes in P21 *TRP1-Cre* and *Pten-cko* littermate mouse RPE were examined by RT-PCR. Relative amounts of total mRNA and the loss of *Pten* gene expression in the samples used for the experiments were determined by RT-PCR of *actinβ1* and of *Pten*, respectively. (B) RT-PCR band intensities were measured by Image-J software and the ratio to the intensity values of *TRP1-Cre* samples are shown in the graph (n = 3, 3 independent litters). (C) Relative levels of Adh1, Adh7, Rdh5, Rdh10, and Rpe65 proteins in *TRP1-Cre* and *Pten-cko* mouse RPE and retina were determined by WB. The concentration of ROL (D) and RA (E) in P21 *TRP1-Cre* and *Pten-cko* mouse RPE (20 mg tissue) and retina (90 mg tissue) were determined by ELISA (see details in Materials and Methods section). Error bars denote SD. n.s., not significant; $*P < 0.05$, $**P < 0.01$, $***P < 0.001$.

However, we found that the numbers of Otx2-positive RPE cells in P50 *at*-RA-injected *Pten-cko* mouse eyes were not significantly different from those observed in the vehicle (i.e., DMSO)-injected groups (Figs. 2A and 2B). Instead, we found that the numbers of rhodopsin-positive photoreceptors in the outer nuclear layer (ONL) were increased in *Pten-cko* mouse retinas without any significant change in the numbers of the cells in the inner nuclear layer (INL) (Figs. 2A and 2B). These results suggest that ectopic *at*-RA does not act as a protective factor for the RPE; instead, consistent with previous reports (Kelley et al., 1994), this treatment appears to protect photoreceptors.

Unexpectedly, we found that the ONL structures of *at*-RA-injected mice were disrupted and formed multiple rosettes regardless of genotype (Fig. 2A). These retinal rosettes have been suggested to arise from the degeneration of Müller glia (MG) (Willbold et al., 2000). Supporting this, Sox2-positive MG cell bodies failed to align properly the INL of rosette areas in *at*-RA-injected *TRP1-Cre* mouse retinas (Fig. 2A, arrowheads), whereas they formed a sharp layer in the middle INL of DMSO-injected retinas. We also found that the RPE of *at*-RA-injected *TRP1-Cre* mice failed to exhibit polarized features, which are necessary for the ability of the RPE to interact with photoreceptor OS and contrib-

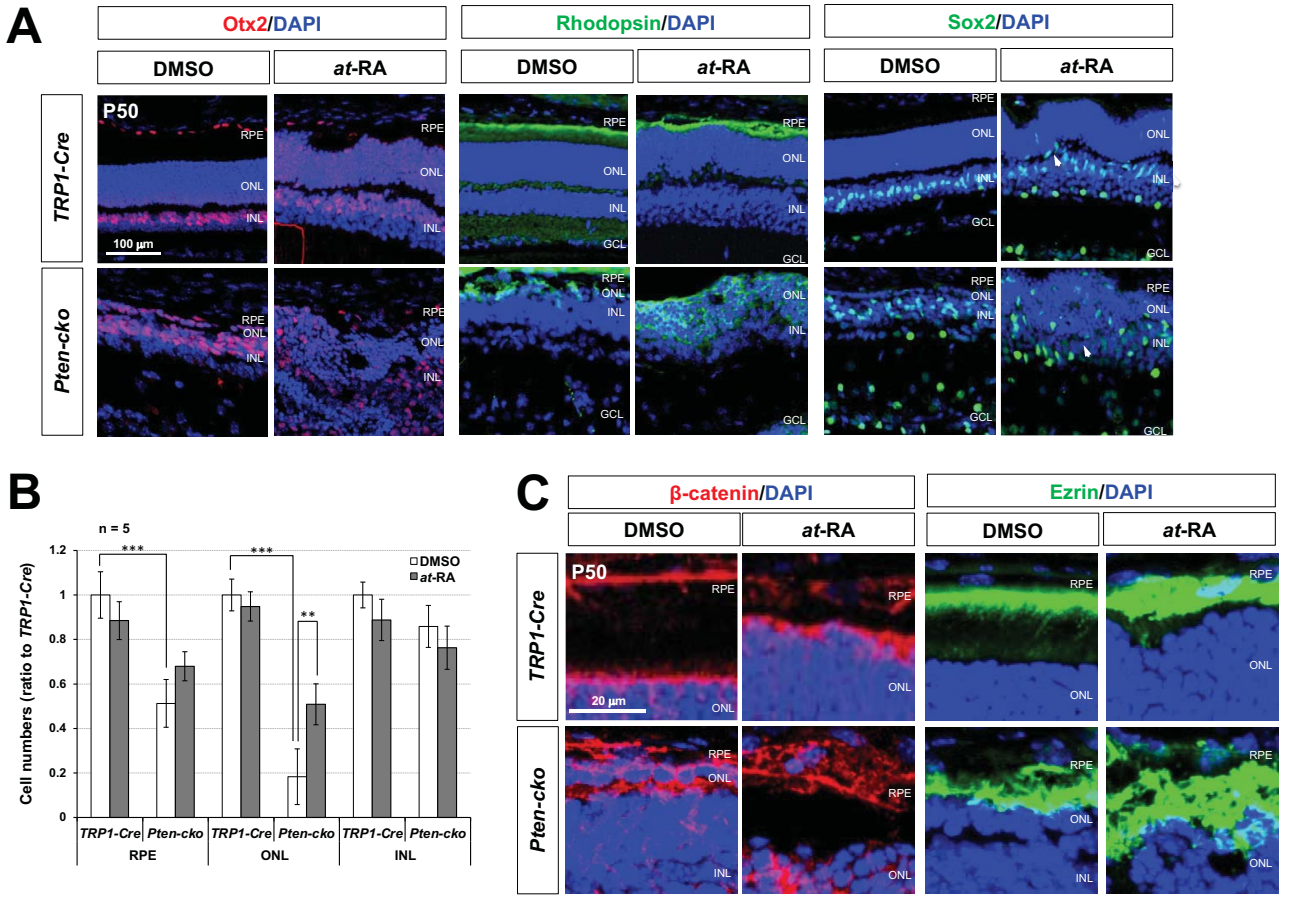

Fig. 2. Degeneration of *Pten*-deficient mouse RPE cannot be rescued by RA supplement. (A) *Pten-cko* and *TRP1-Cre* mice were injected with *at*-RA (20 mg/kg) intraperitoneally at every other day from P21 to P50. The cells expressing specific markers, including Otx2 (positive in RPE, photoreceptor, bipolar cell), Rhod (positive in rod photoreceptors), and Sox2 (positive in MG and amacrine cell subsets), in P50 *Pten-cko* and *TRP1-Cre* mice eye sections were examined by immunohistochemistry (see details in Materials and Methods section). GCL, ganglion cell layer. (B) DAPI-labeled nuclei of RPE, ONL and INL cells were counted and the relative numbers are shown in the graph (n = 5, 5 independent litters). Error bars denote SD. $**P < 0.01$, $***P < 0.001$. (C) Polarity of mouse RPE was determined by immunostaining of β-catenin and ezrin, which are enriched in the basolateral and apical sides of the RPE, respectively.

ute to maintaining the retina-blood barrier function of the RPE (Finnemann and Chang, 2008). β-Catenin, which was enriched in the basolateral sides of the RPE from DMSO-injected *TRP1-Cre* mice, was detected throughout the RPE of *at*-RA-injected *TRP1-Cre* mice with a distribution similar to that seen in *Pten-cko* mouse RPE (Fig. 2C). Ezrin was detected in the apical side of RPE in *TRP1-Cre* mice injected with *at*-RA, but it failed to show the well-organized brush-like distribution pattern seen in DMSO-injected *TRP1-Cre* mouse RPE (Fig. 2C).

Protection of Pten-deficient mouse RPE by feeding of a ROL-free diet

As previous work showed that high-dose ROL is toxic to cells (DiPalma and Ritchie, 1977), we next investigated whether increase of ROL was correlated with the degeneration of *Pten*-deficient mouse RPE. To address this question, we fed mice *ad libitum* from P21 with a chow lacking VitA, which is a natural source of ROL. In contrast to the severely reduced RPE and photoreceptor cell numbers in P50 *Pten-cko* mice fed a ROL-containing normal diet, these numbers in P50 *Pten-cko* mice fed the ROL-free diet were rescued to levels comparable to those observed in P50 *TRP1-Cre* littermate mice (Fig. 3A, Supplementary Fig. S1A). Moreover, the polarized distributions of β-catenin and ezrin to the basolateral and apical sides (Le et al., 2021), respectively, were recovered in the RPE of *Pten*-deficient mice fed the ROL-free diet (Figs. 3A and 3B). These results suggest that a ROL-free diet alleviates the RPE degeneration in *Pten-cko* mice from P21 to P50.

However, the rescued RPE and retinal phenotypes were not maintained in *Pten-cko* mice fed the ROL-free diet for an additional 30 days (to P80) (Figs. 3C and 3D, Supplementary Fig. S1B). Dietary supplement of β-carotene, which can be broken into two RAL molecules for further conversion to ROL and RA (Thompson et al., 2019), was necessary to maintain RPE and retinas intact in *Pten-cko* mice fed a ROL-free chow by P80 (Figs. 3C and 3D, Supplementary Fig. S1B). Together, these results suggest that an elevation of ROL in *Pten*-defi-

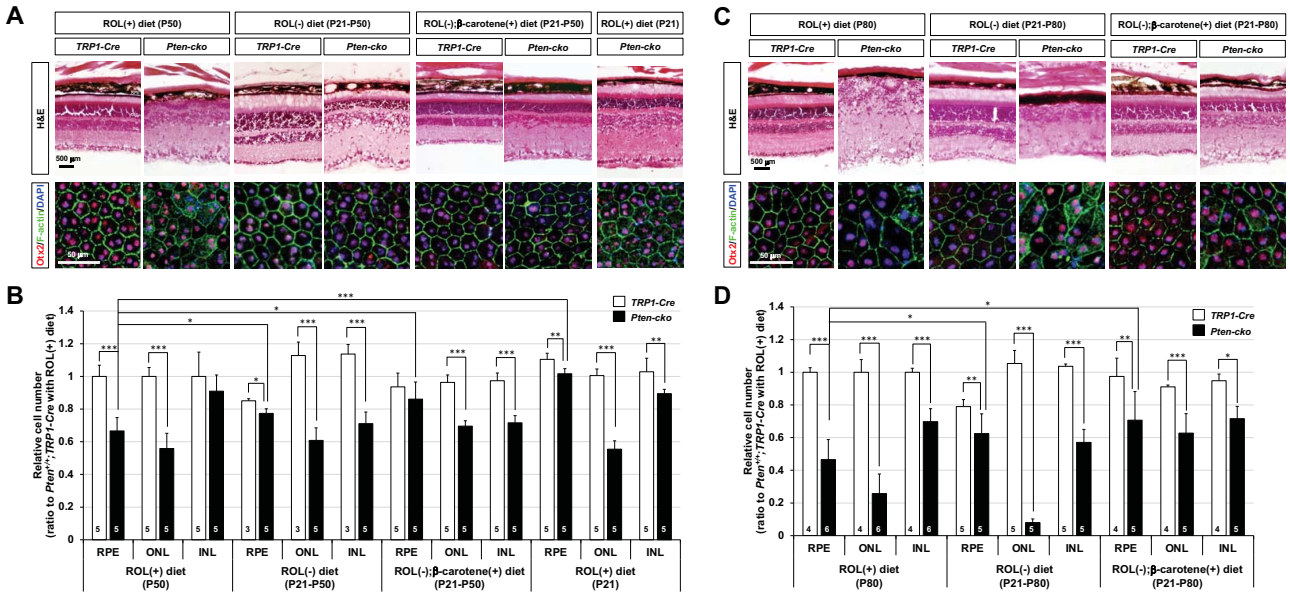

Fig. 3. Dietary restriction of ROL rescues *Pten*-deficient mouse RPE from degeneration. (A and C) *Pten-cko* and *TRP1-Cre* mice were fed normal (ROL(+)), ROL-free (ROL(-)), or β-carotene-supplemented ROL-free (ROL(-);β-carotene) diets from P21 to P50 or P80. Eye and retinal structures of those mice were investigated by H&E staining of the eye sections at P50 (A) or P80 (C). Nuclei and F-actin in mouse RPE were visualized by immunostaining of flat-mount mouse eye cups with anti-Otx2 antibody and staining with phalloidine-Alexa647, respectively. Nuclei of the cells in the eye cups were also visualized by DAPI staining. (B and D) Numbers of cells in the ONL and INL of the retinal sections and numbers of RPE in the flat-mount eye cups were counted and the relative numbers to those in *TRP1-Cre* mice subjected to normal diet were shown in the graphs. Numbers of samples analyzed are shown in the bars of each graph. Error bars denote SD. $*P < 0.05$, $**P < 0.01$, $***P < 0.001$.

cient RPE is likely to be a cause of the observed degeneration.

FoxO transcription factors regulate Adh and Rdh expression in the mouse RPE

To begin identifying the transcription factors responsible for regulating the expression levels of *Adh* and *Rdh* genes exhibited decreased expression the *Pten*-deficient mouse RPE (Figs. 1A-1C), we compared the DNA sequences of various vertebrate *ADH1*, *ADH7*, and *RDH10* genes. We identified conserved DNA sequences located upstream of the transcription initiation sites of these genes (Fig. 4A, yellow highlights). We next isolated the DNA sequences upstream of mouse *Adh1*, *Adh7*, and *Rdh10* genes, cloned them into the pGL3 luciferase reporter vector, and assessed for potential promoter and enhancer activities of the sequences. All of the tested upstream sequences induced meaningful luciferase expression in human embryonic kidney 293T cells (Supplementary Fig. S2A). Given that the *Adh1, Adh7,* and *Rdh10* mRNA were down-regulated in the *Pten*-deficient RPE, which exhibited hyperactive Akt (Figs. 1A and 1B), we next tested whether the luciferase expression driven by the upstream sequences was sensitive to Akt. Indeed, we found the luciferase expression was significantly decreased by co-expression of constitutively active (CA) AKT1 (AKT1(CA)) but not kinase-inactive $AKT1^{K179M}$ (AKT1-KM) (Fig. 4B). These results suggest that the expression levels of the tested *Rdh* genes are induced by transcription factors that are negatively regulated by Akt.

Further analyses of the DNA sequences revealed that they commonly included consensus binding sequences for forkhead box class O (FOXO) transcription factors (Fig. 4A, Supplementary Fig. S2B), which are known to be negatively regulated by Akt-mediated phosphorylation (Brunet et al., 2001). Thus, we performed chromatin immunoprecipitation (ChIP) with an anti-FOXO3a antibody to examine whether FoxO transcription factors could bind the putative forkhead response elements (FHRE) in the upstream sequences of *Adh1*, *Adh7*, and *Rdh10* in the mouse RPE. The obtained results suggested that FoxO3a bound to the FHRE sequences upstream of the analyzed genes in the RPE with an efficiency comparable to that of the well-characterized FHRE of *growth arrest and DNA-damage-inducible-45 α* (*Gadd45a*) (Tran et al., 2002) (Fig. 4C).

Next, we tested whether luciferase expression driven by the upstream sequences could be positively or negatively regulated by FOXO3A. We found that luciferase expression was elevated by co-expression of human FOXO3A (Fig. 4D), and further observed that co-expression of AKT1-CA abolished this effect in the cells expressing FOXO3A but not FOXO3A (T32M) (FOXO3-TM), which is resistant to phosphorylation by AKT (Fig. 4D). These results suggest that FOXO3A positively regulates the expression levels of the analyzed genes and AKT antagonizes this effect.

We found that the mouse RPE expresses all three FoxO isotypes: FoxO1, FoxO3a, and FoxO4 (Fig. 4E). The levels of phosphorylated FoxO1 and FoxO3a were significantly elevated in P21 *Pten*-deficient mouse RPE in comparison to

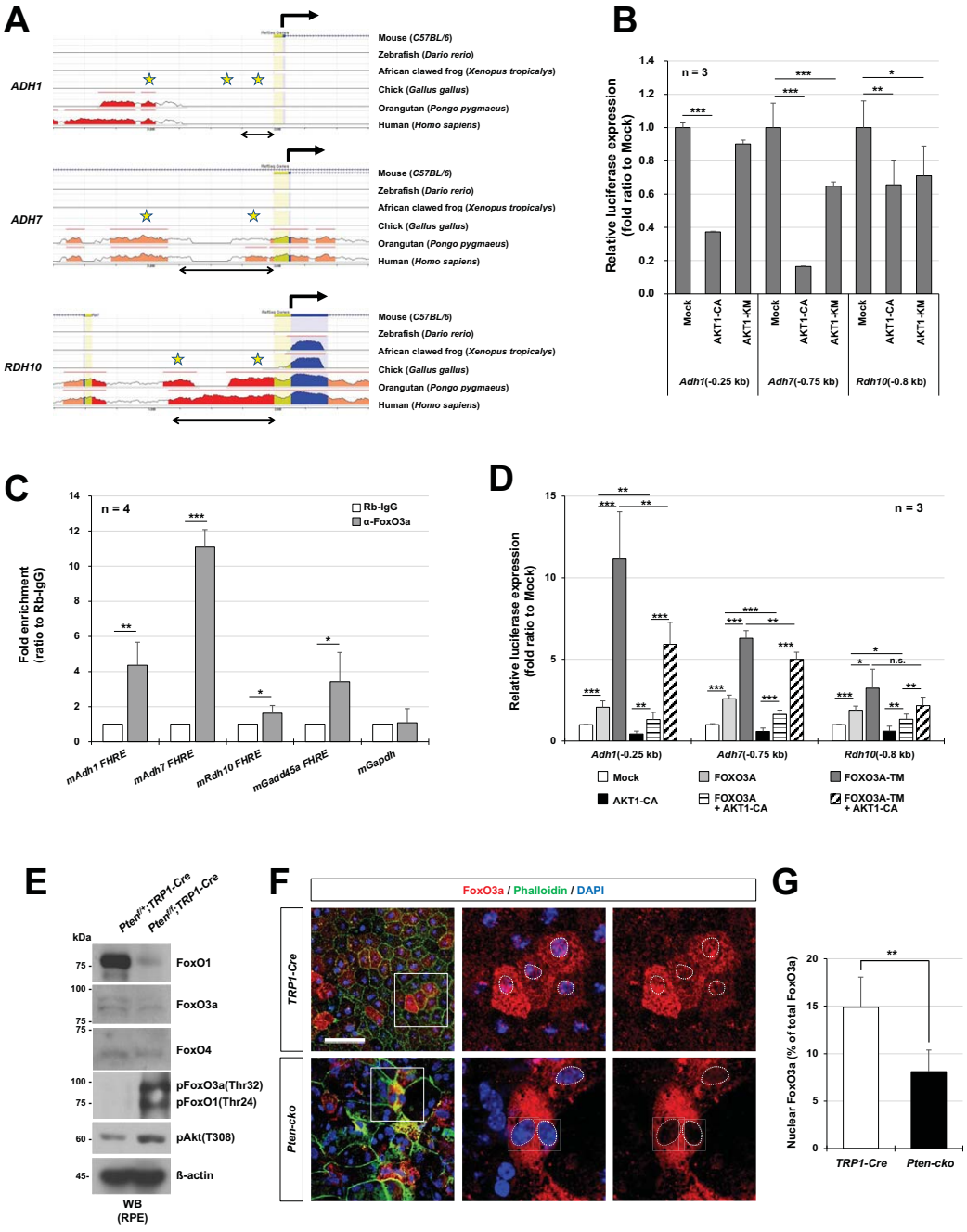

Fig. 4. FoxO regulates *Rdh* expression in mouse RPE. (A) Genomic DNA sequences of mouse *Adh1*, *Adh7*, and *Rdh10* were compared with those of other vertebrate homologous genes and the consensus sequences that can be recognized by FOXO in the upstream of transcription initiation sites are marked by yellow asterisks (see details in Materials and Methods section). (B) pGL3 luciferase reporter constructs containing the upstream sequences of mouse *Adh1*, *Adh7*, and *Rdh10* genes were expressed in 293T cells and the effects of co-expressed AKT1-CA and AKT1-KM on the luciferase expression were examined. (C) DNA fragments that were pulled down from 6 months-old mouse RPE by ChIP with rabbit anti-FOXO3a IgG or pre-immune rabbit IgG. Relative amounts of the upstream sequences of *Adh1*, *Adh7*, and *Rdh10*, which include the FoxO target sequences, in the ChIPed DNA fragments were investigated by RT-qPCR. Numbers of samples analyzed are shown in the bars of each graph. Error bars denote SD. $*P < 0.05$, $**P < 0.01$, $***P < 0.001$. (D) The pGL3 luciferase reporter constructs were co-expressed with wild-type FOXO3A or FOXO3A-TM mutant, which is resistant to Akt-mediated phosphorylation, and the effects of those FOXO3A variants on the luciferase expression were examined. Error bars denote SD. n.s., not significant. (E) Relative amounts of FoxO1, FoxO3a, FoxO4, pFoxO1(Thr24)/pFoxO3a(Thr32), and pAkt(T308) in P21 *TRP1-Cre* and *Pten-cko* littermate mouse RPE were investigated by WB with the antibodies detecting the corresponding proteins. (F) Subcellular distribution of FoxO3a in P21 *TRP1-Cre* and *Pten-cko* mice RPE was investigated by immunostaining. Nuclei and F-actin in mouse RPE was visualized by staining with DAPI (blue) and phalloidin-Alexa647 dyes (green), respectively. Scale bar = 50 μm.

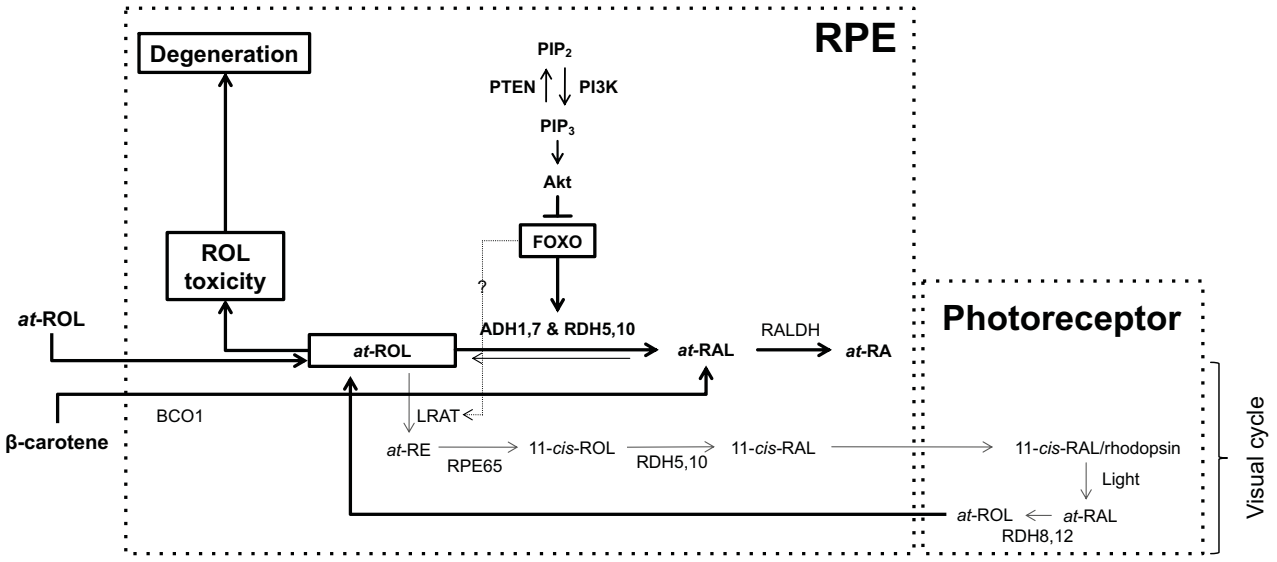

Fig. 5. Diagram depicts the regulation of retinoid metabolism by PI3K-AKT pathway in RPE. RPE expresses RDHs, including ADH1,7 and RDH5,10, to convert ROL to RAL, and vice versa. In *PTEN*-deficient RPE, AKT is activated to inactivate FOXO, resulting in the decrease of RDH expression. Consequently, *at*-ROL, which is taken up from photoreceptors through retinol visual cycle and/or supplied in diet, is accumulated in the RPE to cause the toxicity. Therefore, dietary replacement of *at*-ROL to β-carotene, which can be converted to *at*-RAL, can protect RPE from the ROL toxicity-induced degeneration.

TRP1-Cre littermate mouse RPE (Fig. 4E), suggesting that FoxO1 and FoxO3a undergo Akt-mediated phosphorylational inactivation in the *Pten*-deficient mouse RPE. Furthermore, the cytoplasmic retention of FoxO3a, which is induced by Akt-mediated phosphorylation (Brunet et al., 1999), was enhanced in the *Pten*-deficient mouse RPE (Fig. 4F). These results suggest that hyperactive Akt in the *Pten*-deficient RPE might inhibit the expression of *Adh* and *Rdh* genes via the phosphorylation and remobilization of FoxO transcription factors from the nucleus to the cytoplasm. This could lead to the toxic accumulation of ROL in the RPE, which could be rescued by dietary replacement of VitA and β-carotene (Fig. 5).

DISCUSSION

Given that the mammalian visual system uses 11-*cis*-RAL as a functional photopigment, proper retinoid metabolism in the photoreceptor and RPE is necessary for proper vision. In support of this, many forms of congenital blindness and early onset retinal degenerative disease, including LCA, Stargardt disease, cone-rod dystrophy, and RP, are associated with mutations in retinoid metabolism genes (Morimura et al., 1998). Among the enzymes involved in retinoid metabolism, LRAT (which converts *at*-ROL to *at*-RE) and RPE65 (which isomerizes *at*-ROL to 11-*cis*-ROL) are expressed exclusively in the RPE, suggesting that the RPE plays crucial roles in retinoid metabolism (Redmond et al., 1998; Saari et al., 1993). Consequently, the substrates of those enzymes (*at*-ROL and *at*-RE) are accumulated in the RPE of *Lrat*- and *Rpe65*-deficient mice, respectively (Imanishi et al., 2004). Dietary supply of *at*-ROL to *Lrat*-deficient mice, therefore, should elevate *at*-ROL in the mouse RPE to a toxic level. Fortunately, *at*-ROL can be metabolized to *at*-RAL by RDHs, which are also enriched in the RPE (Figs. 1A and 1B). This enables the RPE to persist in mice lacking *Lrat* (Ruiz et al., 2007). Therefore, combinatorial mutations of retinoid metabolic enzymes expressed in the RPE might be needed to induce RPE degeneration and the associated retinal degenerative diseases.

Here, we suggest that *Pten* deficiency elevates ROL via the reduced expression of *Rdh* genes in mouse RPE, and that this appears to trigger degeneration of the RPE (Figs. 1D and 3A). Excessive ROL was reported to activate monoamine oxidase enzyme (MAO) and subsequently increase the level of hydrogen peroxide (H_2O_2) to disrupt mitochondrial redox maintenance (de Oliveira et al., 2012; Richter et al., 1995). Thus, the elevation of ROL in the *Pten*-deficient mouse RPE might also induce mitochondrial dysfunction, which was shown to induce RPE degeneration (Brown et al., 2019). However, additional studies are needed to more precisely define the mechanisms of ROL toxicity in the *Pten*-deficient mouse RPE.

Our results indicate that dietary restriction of ROL can delay the degeneration of the *Pten*-deficient mouse RPE in the short term (Figs. 3A and 3B). However, the RPE did not persist under longer-term feeding of the ROL-free diet (Figs. 3C and 3D), suggesting that an alternative source of ROL should be supplied. ROL and RA can be produced from β-carotene-derived RAL by RDH and RALDH, respectively, and could be utilized by mice in the absence of a dietary supply of ROL (Kim et al., 2011). Thus, we supplied β-carotene to *Pten-cko* mice being fed the ROL-free chow, and found that this protected the RPE over the longer term (Figs. 3C and 3D).

Dietary supplementation of β-carotene (β,β-carotene) and other carotenoids, such as lutein/zeaxanthin (β,ε-carotene-

3,3'-diol) and lycopene (ψ,ψ-carotene), has long been recommended to support healthy vision (Krinsky and Johnson, 2005). β-Carotene is also known to have anti-oxidative, anti-cancer, and anti-obesity activities (Nagao, 2009). However, excessive intake of β-carotene can cause other health problems, including a yellowish discoloration of the skin (Hess and Myers, 1919). Interventional trials also found that high doses of β-carotene could have negative effects on the incidence of lung cancer and cardiovascular diseases in smokers (Alpha-Tocopherol, Beta Carotene Cancer Prevention Study Group, 1994; Omenn et al., 1996). Thus, it should be provided at an optimal concentration.

Previous reports indicated that FOXO1 regulates *Rdh1*, *Rdh8*, and *Rdh10* but the physiological relevance of FOXO-dependent *Rdh* gene expression remained unknown. Here, we show that FoxO3a binds to well-conserved FOXO-binding sequences upstream of *Adh1, Adh7,* and *Rdh10* to induce the expression of these transcripts in the mouse RPE (Fig. 4C). We further identified that FoxO-dependent regulation of *Rdh* gene expression is sensitive to Pten-Akt signaling (Figs. 4D-4G). Similar to the pathogenic output of Pten inactivation in the mouse RPE (Kim et al., 2008; Lee et al., 2011), ROL toxicity could account for the degeneration of other tissues in which FoxO activity is reduced by Akt or other negative regulators (Fig. 5). Additional studies are therefore needed to investigate whether FoxO transcription factors are major regulators of *Rdh* expression *in vivo*.

Note: Supplementary information is available on the Molecules and Cells website (www.molcells.org).

ACKNOWLEDGMENTS

This work was supported by the National Research Foundation of Korea (NRF) grants funded by Korean Ministry of Science and ICT (MSIT) (2017R1A2B3002862 and 2018R1A5A1024261; J.W.K.); the grant funded by Samsung Foundation of Science and Technology (SSTF-BA1802-10; J.W.K.).

AUTHOR CONTRIBUTIONS

Y.J.K. conceived and performed experiments, and wrote the manuscript. S.P., T.H., S.K., S.L., and H.Y. performed experiments. J.W.K. conceived and supervised the experiments, wrote the manuscript, and secured funding.

CONFLICT OF INTEREST

The authors have no potential conflicts of interest to disclose.

ORCID

You-Joung Kim	https://orcid.org/0000-0003-4089-8292
Sooyeon Park	https://orcid.org/0000-0001-5357-2342
Taejeong Ha	https://orcid.org/0000-0003-1664-1593
Seungbeom Kim	https://orcid.org/0000-0002-7540-3344
Soyeon Lim	https://orcid.org/0000-0003-3106-2282
Han You	https://orcid.org/0000-0003-1481-5465
Jin Woo Kim	https://orcid.org/0000-0003-0767-1918

REFERENCES

Alpha-Tocopherol, Beta Carotene Cancer Prevention Study Group (1994). The effect of vitamin E and beta carotene on the incidence of lung cancer and other cancers in male smokers. N. Engl. J. Med. *330*, 1029-1035.

Bainbridge, J.W., Smith, A.J., Barker, S.S., Robbie, S., Henderson, R., Balaggan, K., Viswanathan, A., Holder, G.E., Stockman, A., Tyler, N., et al. (2008). Effect of gene therapy on visual function in Leber's congenital amaurosis. N. Engl. J. Med. *358*, 2231-2239.

Brown, E.E., DeWeerd, A.J., Ildefonso, C.J., Lewin, A.S., and Ash, J.D. (2019). Mitochondrial oxidative stress in the retinal pigment epithelium (RPE) led to metabolic dysfunction in both the RPE and retinal photoreceptors. Redox Biol. *24*, 101201.

Brunet, A., Bonni, A., Zigmond, M.J., Lin, M.Z., Juo, P., Hu, L.S., Anderson, M.J., Arden, K.C., Blenis, J., and Greenberg, M.E. (1999). Akt promotes cell survival by phosphorylating and inhibiting a Forkhead transcription factor. Cell *96*, 857-868.

Brunet, A., Datta, S.R., and Greenberg, M.E. (2001). Transcription-dependent and -independent control of neuronal survival by the PI3K-Akt signaling pathway. Curr. Opin. Neurobiol. *11*, 297-305.

Cunningham, T.J. and Duester, G. (2015). Mechanisms of retinoic acid signalling and its roles in organ and limb development. Nat. Rev. Mol. Cell Biol. *16*, 110-123.

de Oliveira, M.R., da Rocha, R.F., Pasquali, M.A.d.B., and Moreira, J.C.F. (2012). The effects of vitamin A supplementation for 3 months on adult rat nigrostriatal axis: Increased monoamine oxidase enzyme activity, mitochondrial redox dysfunction, increased β-amyloid1–40 peptide and TNF-α contents, and susceptibility of mitochondria to an in vitro H_2O_2 challenge. Brain Res. Bull. *87*, 432-444.

DiPalma, J.R. and Ritchie, D.M. (1977). Vitamin toxicity. Ann. Rev. Pharmacol. Toxicol. *17*, 133-148.

Ferreira, R., Napoli, J., Enver, T., Bernardino, L., and Ferreira, L. (2020). Advances and challenges in retinoid delivery systems in regenerative and therapeutic medicine. Nat. Commun. *11*, 4265.

Finnemann, S.C. and Chang, Y. (2008). Photoreceptor—RPE interactions. In Visual Transduction and Non-Visual Light Perception, J. Tombran-Tink and C.J. Barnstable, eds. (Totowa, NJ: Humana Press), pp. 67-86.

Garita-Hernandez, M., Lampic, M., Chaffiol, A., Guibbal, L., Routet, F., Santos-Ferreira, T., Gasparini, S., Borsch, O., Gagliardi, G., Reichman, S., et al. (2019). Restoration of visual function by transplantation of optogenetically engineered photoreceptors. Nat. Commun. *10*, 4524.

Hess, A.F. and Myers, V.C. (1919). Carotinemia: a new clinical picture. JAMA *73*, 1743-1745.

Imanishi, Y., Batten, M.L., Piston, D.W., Baehr, W., and Palczewski, K. (2004). Noninvasive two-photon imaging reveals retinyl ester storage structures in the eye. J. Cell Biol. *164*, 373-383.

Jin, M., Li, S., Moghrabi, W.N., Sun, H., and Travis, G.H. (2005). Rpe65 is the retinoid isomerase in bovine retinal pigment epithelium. Cell *122*, 449-459.

Kang, K.H., Lemke, G., and Kim, J.W. (2009). The PI3K-PTEN tug-of-war, oxidative stress and retinal degeneration. Trends Mol. Med. *15*, 191-198.

Kelley, M.W., Turner, J.K., and Reh, T.A. (1994). Retinoic acid promotes differentiation of photoreceptors in vitro. Development *120*, 2091-2102.

Kim, J.W., Kang, K.H., Burrola, P., Mak, T.W., and Lemke, G. (2008). Retinal degeneration triggered by inactivation of PTEN in the retinal pigment epithelium. Genes Dev. *22*, 3147-3157.

Kim, Y.K., Wassef, L., Chung, S., Jiang, H., Wyss, A., Blaner, W.S., and Quadro, L. (2011). β-Carotene and its cleavage enzyme β-carotene-15,15'-oxygenase (CMOI) affect retinoid metabolism in developing tissues. FASEB J. *25*, 1641-1652.

Krinsky, N.I. and Johnson, E.J. (2005). Carotenoid actions and their relation

to health and disease. Mol. Aspects Med. *26*, 459-516.

Le, D., Lim, S., Min, K.W., Park, J.W., Kim, Y., Ha, T., Moon, K.H., Wagner, K.U., and Kim, J.W. (2021). Tsg101 is necessary for the establishment and maintenance of mouse retinal pigment epithelial cell polarity. Mol. Cells *44*, 168-178.

Lee, E.J., Kim, N., Kang, K.H., and Kim, J.W. (2011). Phosphorylation/inactivation of PTEN by Akt-independent PI3K signaling in retinal pigment epithelium. Biochem. Biophys. Res. Commun. *414*, 384-389.

Leid, M., Kastner, P., and Chambon, P. (1992). Multiplicity generates diversity in the retinoic acid signalling pathways. Trends Biochem. Sci. *17*, 427-433.

Liden, M. and Eriksson, U. (2006). Understanding retinol metabolism: structure and function of retinol dehydrogenases. J. Biol. Chem. *281*, 13001-13004.

Maden, M. (2002). Retinoid signalling in the development of the central nervous system. Nat. Rev. Neurosci. *3*, 843-853.

Michalik, L. and Wahli, W. (2007). Guiding ligands to nuclear receptors. Cell *129*, 649-651.

Moon, K.H., Kim, H.T., Lee, D., Rao, M.B., Levine, E.M., Lim, D.S., and Kim, J.W. (2018). Differential expression of NF2 in neuroepithelial compartments is necessary for mammalian eye development. Dev. Cell *44*, 13-28.e3.

Morimura, H., Fishman, G.A., Grover, S.A., Fulton, A.B., Berson, E.L., and Dryja, T.P. (1998). Mutations in the RPE65 gene in patients with autosomal recessive retinitis pigmentosa or leber congenital amaurosis. Proc. Natl. Acad. Sci. U. S. A. *95*, 3088-3093.

Nagao, A. (2009). Absorption and function of dietary carotenoids. Forum Nutr. *61*, 55-63.

Niederreither, K. and Dolle, P. (2008). Retinoic acid in development: towards an integrated view. Nat. Rev. Genet. *9*, 541-553.

Obsil, T. and Obsilova, V. (2011). Structural basis for DNA recognition by FOXO proteins. Biochim. Biophys. Acta *1813*, 1946-1953.

Omenn, G.S., Goodman, G.E., Thornquist, M.D., Balmes, J., Cullen, M.R., Glass, A., Keogh, J.P., Meyskens, F.L., Valanis, B., Williams, J.H., et al. (1996). Effects of a combination of beta carotene and vitamin A on lung cancer and cardiovascular disease. N. Engl. J. Med. *334*, 1150-1155.

Pares, X., Farres, J., Kedishvili, N., and Duester, G. (2008). Medium- and short-chain dehydrogenase/reductase gene and protein families: medium-chain and short-chain dehydrogenases/reductases in retinoid metabolism. Cell. Mol. Life Sci. *65*, 3936-3949.

Parish, C.A., Hashimoto, M., Nakanishi, K., Dillon, J., and Sparrow, J. (1998). Isolation and one-step preparation of A2E and iso-A2E, fluorophores from human retinal pigment epithelium. Proc. Natl. Acad. Sci. U. S. A. *95*, 14609-14613.

Putting, B.J., Zweypfenning, R.C., Vrensen, G.F., Oosterhuis, J.A., and van Best, J.A. (1992). Blood-retinal barrier dysfunction at the pigment epithelium induced by blue light. Invest. Ophthalmol. Vis. Sci. *33*, 3385-3393.

Radu, R.A., Mata, N.L., Bagla, A., and Travis, G.H. (2004). Light exposure stimulates formation of A2E oxiranes in a mouse model of Stargardt's macular degeneration. Proc. Natl. Acad. Sci. U. S. A. *101*, 5928-5933.

Redmond, T.M., Yu, S., Lee, E., Bok, D., Hamasaki, D., Chen, N., Goletz, P., Ma, J.X., Crouch, R.K., and Pfeifer, K. (1998). Rpe65 is necessary for production of 11-cis-vitamin A in the retinal visual cycle. Nat. Genet. *20*, 344-351.

Richter, C., Gogvadze, V., Laffranchi, R., Schlapbach, R., Schweizer, M., Suter, M., Walter, P., and Yaffee, M. (1995). Oxidants in mitochondria: from physiology to diseases. Biochim. Biophys. Acta *1271*, 67-74.

Ruiz, A., Ghyselinck, N.B., Mata, N., Nusinowitz, S., Lloyd, M., Dennefeld, C., Chambon, P., and Bok, D. (2007). Somatic ablation of the Lrat gene in the mouse retinal pigment epithelium drastically reduces its retinoid storage. Invest. Ophthalmol. Vis. Sci. *48*, 5377-5387.

Saari, J.C. and Bredberg, D.L. (1989). Lecithin:retinol acyltransferase in retinal pigment epithelial microsomes. J. Biol. Chem. *264*, 8636-8640.

Saari, J.C., Bredberg, D.L., and Farrell, D.F. (1993). Retinol esterification in bovine retinal pigment epithelium: reversibility of lecithin:retinol acyltransferase. Biochem. J. *291* (Pt 3), 697-700.

Sahu, B. and Maeda, A. (2016). Retinol dehydrogenases regulate vitamin A metabolism for visual function. Nutrients *8*, 746.

Sommer, A. (2008). Vitamin a deficiency and clinical disease: an historical overview. J. Nutr. *138*, 1835-1839.

Stambolic, V., Suzuki, A., de la Pompa, J.L., Brothers, G.M., Mirtsos, C., Sasaki, T., Ruland, J., Penninger, J.M., Siderovski, D.P., and Mak, T.W. (1998). Negative regulation of PKB/Akt-dependent cell survival by the tumor suppressor PTEN. Cell *95*, 29-39.

Thompson, B., Katsanis, N., Apostolopoulos, N., Thompson, D.C., Nebert, D.W., and Vasiliou, V. (2019). Genetics and functions of the retinoic acid pathway, with special emphasis on the eye. Hum. Genomics *13*, 61.

Tran, H., Brunet, A., Grenier, J.M., Datta, S.R., Fornace, A.J., Jr., DiStefano, P.S., Chiang, L.W., and Greenberg, M.E. (2002). DNA repair pathway stimulated by the forkhead transcription factor FOXO3a through the Gadd45 protein. Science *296*, 530-534.

von Lintig, J. and Vogt, K. (2000). Filling the gap in vitamin A research. Molecular identification of an enzyme cleaving beta-carotene to retinal. J. Biol. Chem. *275*, 11915-11920.

Willbold, E., Rothermel, A., Tomlinson, S., and Layer, P.G. (2000). Müller glia cells reorganize reaggregating chicken retinal cells into correctly laminated in vitro retinae. Glia *29*, 45-57.